



HAL
open science

Investigation of Na⁺ and K⁺ transport in halophytes: Functional analysis of the HmHKT2;1 transporter from Hordeum maritimum and expression under saline conditions

Dorsaf Hmidi, Dorsa Messedi, Claire Corratgé-Faillie, Théo Marhuenda, Cécile Fizames, Walid Zorrig, Chedly Abdelly, Herve Sentenac, Anne-Aliénor Véry

► To cite this version:

Dorsaf Hmidi, Dorsa Messedi, Claire Corratgé-Faillie, Théo Marhuenda, Cécile Fizames, et al.. Investigation of Na⁺ and K⁺ transport in halophytes: Functional analysis of the HmHKT2;1 transporter from *Hordeum maritimum* and expression under saline conditions. *Plant and Cell Physiology*, 2019, 60 (11), pp.2423-2435. 10.1093/pcp/pcz136 . hal-02623588

HAL Id: hal-02623588

<https://hal.inrae.fr/hal-02623588>

Submitted on 10 Aug 2022

HAL is a multi-disciplinary open access archive for the deposit and dissemination of scientific research documents, whether they are published or not. The documents may come from teaching and research institutions in France or abroad, or from public or private research centers.

L'archive ouverte pluridisciplinaire **HAL**, est destinée au dépôt et à la diffusion de documents scientifiques de niveau recherche, publiés ou non, émanant des établissements d'enseignement et de recherche français ou étrangers, des laboratoires publics ou privés.

Investigation of Na⁺ and K⁺ transport in halophytes: Functional analysis of the HmHKT2;1 transporter from *Hordeum maritimum* and expression under saline conditions

Running title: HKT2;1 transporter from *Hordeum maritimum*

Corresponding author:

A.-A. Véry

Biochimie et Physiologie Moléculaire des Plantes, Univ Montpellier, CNRS, INRA, SupAgro
Montpellier, Campus SupAgro-INRA, 34060 Montpellier Cedex 2, France

Tel: +33 4 99 61 25 74

Fax: +33 4 67 52 57 37

e-mail very@supagro.inra.fr

Subject area: (7) membrane and transport

9 black and white Figures

Supplementary material: 8 black and white Figures and 2 Tables

Investigation of Na⁺ and K⁺ transport in halophytes: Functional analysis of the HmHKT2;1 transporter from *Hordeum maritimum* and expression under saline conditions

Running title: HKT2;1 transporter from *Hordeum maritimum*

Dorsaf Hmidi^{1,2}, Dorsaf Messedi², Claire Corratgé-Faillie¹, Théo Marhuenda¹, Cécile Fizames¹, Walid Zorrig², Chedly Abdelly², Hervé Sentenac¹, Anne-Aliénor Véry^{1,*}

¹*Biochimie et Physiologie Moléculaire des Plantes, Univ Montpellier, CNRS, INRA, SupAgro Montpellier, Campus SupAgro-INRA, 34060 Montpellier Cedex 2, France*

²*Laboratoire des Plantes Extrêmophiles, BP 901, Centre de Biotechnologie, Technopole de Borj Cédria, Hammam-Lif 2050, Tunisia*

* For correspondence (e-mail very@supagro.inra.fr).

Abstract

Control of K⁺ and Na⁺ transport plays a central role in plant adaptation to salinity. In the halophyte *Hordeum maritimum*, we have characterized a transporter gene, named *HmHKT2;1*, whose homologue *HvHKT2;1* in cultivated barley, *Hordeum vulgare*, was known to give rise to increased salt tolerance when overexpressed. The encoded protein is strictly identical in two *H. maritimum* ecotypes, from two biotopes (Tunisian sebkhas) affected by different levels of salinity. These two ecotypes were found to display distinctive responses to salt stress in terms of biomass production, Na⁺ contents, K⁺ contents and K⁺ absorption efficiency. Electrophysiological analysis of *HmHKT2;1* in *Xenopus* oocytes revealed distinctive properties when compared to *HvHKT2;1* and other transporters from the same group, especially a much higher affinity for both Na⁺ and K⁺, and a Na⁺-K⁺ symporter behavior in a very broad range of Na⁺ and K⁺ concentrations, due to reduced K⁺ blockage of the transport pathway. Domain swapping experiments identified the region including the 5th transmembrane segment and the adjacent extracellular loop as playing a major role in the determination of the affinity for Na⁺ and the level of K⁺ blockage in these HKT2;1 transporters. Analysis (qRT-PCR) of *HmHKT2;1* expression in the two ecotypes submitted to saline conditions revealed that the levels of *HmHKT2;1* transcripts was maintained constant in the most salt tolerant ecotype while they decreased in the less tolerant one. Both the unique functional properties of *HmHKT2;1* and the regulation of the expression of the encoding gene could contribute to *H. maritimum* adaptation to salinity.

Keywords: *Hordeum maritimum*, *Hordeum vulgare*, sebkha, salt tolerance, HKT transporter, sodium and potassium transport, structure-function analysis

Introduction

Natural soil salinity and soil salinization due to irrigation with poor quality water challenge agriculture in very large areas of lands under arid and semi-arid climate. High soil salinity is considered to be the main abiotic stress, after drought, which impacts crop production. Most crop plants being poorly tolerant to salt stress (Munns and Tester, 2008), analysis of the mechanisms involved in adaptation to high saline conditions is thus a highly active field of research, aiming at providing information for conventional breeding programs or biotechnological approaches, taking advantage of the characterization of candidate genes (Gaxiola et al. 2001, Yokoi et al. 2002, Mitsuya et al. 2005, Zhao et al. 2006, Chen et al. 2007, Saadia et al. 2013) or of QTL/genetic screen analysis (Shi et al. 2000, Berthomieu et al. 2003, Shi et al. 2003, Ren et al. 2005, James et al. 2011). *Arabidopsis* and rice, which are salt sensitive species, have provided a large part of the knowledge gained in this domain of plant biology.

Adaptation to salinity involves numerous, complex and integrated functions, whose relative importance varies between species, including specific adaptations in some plants, such as succulence or salt excretion by salt glands at the leaf surface (Greenway and Munns 1980, Hasegawa et al. 2000, Munns and Tester 2008, Deinlein et al. 2014). Evidence is however available that, despite the complexity and diversity in adaptation mechanisms, a common determinant of tolerance is the capacity, under high Na^+ concentrations, to efficiently control Na^+ and K^+ uptake and long distance transport and accumulation.

K^+ and Na^+ have very different distributions and roles in the plant. K^+ is an essential element and the most abundant inorganic cation in the cytosol, where it is involved in electrical neutralization of inorganic and organic anions and macromolecules, pH homeostasis, control of membrane electrical potential, activation of enzymes, protein synthesis, cell metabolism, photosynthesis and regulation of cell osmotic pressure (Nieves-Cordones et al. 2016). Through the latter function, it plays a role in turgor-driven cell and organ movements. Thus, plant growth requires large amounts of K^+ ions. In contrast, Na^+ is not an essential element in most plants, except in some halophytes (Flowers 1985). This cation can however be accumulated at high concentrations in vacuoles, where it is used as cheap

osmoticum (Yokoi et al. 2002). Due to this possibility, it can be considered a beneficial element, allowing plants to adjust their water potential when they are facing saline conditions (Niu et al. 1995) and/or to save K^+ for cytosolic uses when the availability of this cation is limiting (Horie et al., 2007). However, the presence of Na^+ in the cytoplasm at high concentrations results in deleterious effects on cell metabolism, *e.g.*, on photosynthetic activity. The use of Na^+ as osmoticum thus requires tight control of Na^+ uptake, long distance transport and compartmentalization at tissue and cell levels. Furthermore, when present at high concentrations in the external medium, Na^+ can both directly interfere with K^+ transporters, due to structural similarities between these two cations, and indirectly affect K^+ transport by strongly depolarizing the cell membrane, thus reducing the driving force for K^+ uptake (Nieves-Cordones et al. 2010).

Several major salt-tolerance QTL identified in different species have been shown to correspond to members from a family of transporters named HKT (acronym of "High Affinity K^+ Transporters") (Ren et al. 2005, Huang et al. 2006, Byrt et al. 2007, Asins et al. 2013, Hamamoto et al. 2015, Campbell et al. 2017, Hartley et al. 2019). For instance, in rice, the SalTol locus, which corresponds to a major salt tolerance QTL (Thomson et al. 2010), contains a member from the HKT family, OsHKT1;5. SalTol seems presently to be the single QTL that is actually used by plant breeders to improve salt tolerance in rice (Singh et al. 2018).

Based on their capacity to transport K^+ and/or Na^+ and phylogenetic analyses, HKT transporters can be sorted in two subfamilies. Subfamily 1 gathers transporters strongly selective for Na^+ (not significantly permeable to K^+), and subfamily 2, transporters permeable to both Na^+ and K^+ (Platten et al. 2006, Corratgé-Faillie et al. 2010). Evidence has been obtained that HKT transporters from subfamily 1 play major roles in plant adaptation to saline conditions by controlling Na^+ long distance transport within the plant vasculature, where they contribute to Na^+ retrieval from the ascending xylem sap flux, and/or to Na^+ recirculation from shoots to roots via the phloem sap (Berthomieu et al. 2003, Ren et al. 2005, Hauser and Horie 2010, Suzuki et al. 2016). Much less information is available for transporters from HKT subfamily 2 and their possible involvement in plant adaptation to saline conditions. However, in cultivated barley, *H. vulgare*, it has been shown that

overexpression of *HvHKT2;1*, a member from HKT subfamily 2, results in increased tolerance to salinity (Mian et al. 2011). Here, we investigate the functional properties of a counterpart of *HvHKT2;1* in the halophyte *Hordeum maritimum*. We used two ecotypes from this species, Soliman and Kalbia, whose biotopes are significantly different with respect to the level of salinity. *H. maritimum* is an annual Poaceae frequently associated with perennial tufts of strict halophytes growing in saline environments, *e.g.*, in depressions named sebkhas in North Africa (Cuénod et al. 1954, Abdelly et al. 2006). The electrical conductivity is close to 20 dS/m in Soliman sebkha (Rabhi et al. 2009), and can reach much higher values, up to 90 dS/m in Kalbia sebkha (Hachicha 2007).

Results

Identification of a homologue of HvHKT2;1 in *Hordeum maritimum*

PCR experiments were carried out, both in the Soliman and Kalbia ecotypes, to clone a *H. maritimum* homologue of *HvHKT2;1*. Cloned cDNAs (GenBank accession number for the Kalbia ecotype: MH019217) were found to encode the same polypeptide in both ecotypes (Supplementary Fig. S1). This transporter was named HmHKT2;1. It displays 18 amino acid changes when compared with HvHKT2;1 (Fig. 1).

HKT transporters display a typical hydrophobic core (Fig. 1A), comprised of 4 successively arranged MPM domains, each of them displaying a so-called Pore region flanked by two transmembrane segments, MPM being the acronym of transMembrane segment, Pore, transMembrane segment (Durell et al. 1999, Kato et al. 2001, Corratgé-Faillie et al. 2010; Hamamoto et al. 2015). The 4 MPM domains are assembled to form the functional hydrophobic core of the protein with a fourfold radial symmetry so that the four P domains are associated at the center of the protein where they structure the ion permeation pathway. Interestingly, 6 from the 18 amino acid differences between HmHKT2;1 and HvHKT2;1 are located in the region lying between residues 320 and 356 (less than 7% of the polypeptide chain; Fig. 1A, B; Supplementary Fig. S1), which corresponds to the first transmembrane segment and the beginning of the P domain of the third MPM domain, suggesting that HmHKT2;1 displays distinctive ion permeation properties, when compared with HvHKT2;1.

The HmHKT2;1 phylogenetic relationships with members from the rice HKT family, HvHKT2,1 from *H. vulgare* (Haro et al. 2005) and TaHKT2;1 from wheat (Rubio et al. 1995, Gassmann et al. 1996), are displayed in Fig. 1C. This analysis identified HmHKT2;1 as a member of HKT subfamily 2 (Platten et al. 2006). All the different members from this subfamily characterized so far have been shown to encode transporters permeable to both Na⁺ and K⁺ when heterologously expressed (Véry et al. 2014).

Comparison of HmHKT2;1 and HvHKT2;1 Na⁺ transport activity in oocytes

Two-electrode voltage-clamp experiments were carried out in *Xenopus* oocytes used as heterologous expression system, in order to analyse the functional properties of HmHKT2;1 and to compare them with those of its *H. vulgare* homologue HvHKT2;1 (Mian et al. 2011).

Oocytes were injected with *HmHKT2;1* or *HvHKT2;1* cRNA or with water (control oocytes). For current recordings, in a first set of experiments, the oocytes were successively bathed in solutions containing different concentrations of Na⁺, from 0.03 to 30 mM, in presence of a fixed concentration of K⁺, 0.5 mM. Representative current traces recorded in 30 mM Na⁺ solution in control oocytes or oocytes expressing HmHKT2;1 or HvHKT2;1 are displayed in Fig. 2B, C and D, respectively. Control oocytes displayed very low current levels in the whole range of imposed membrane potentials (from -15 to -165 mV; Fig. 2A), when compared with oocytes expressing HmHKT2;1 or HvHKT2;1. Current-voltage (I-V) curves obtained from these experiments at the different tested Na⁺ concentrations are displayed by Fig. 2E and F for HmHKT2;1 and HvHKT2;1, respectively. These I-V curves show that, in both HmHKT2;1-and HvHKT2;1-expressing oocytes, the zero current potential (also named reversal potential: E_{rev}) was shifted towards more positive potentials when the external concentration of Na⁺ was increased (see also Fig. 5A). These results demonstrated that HmHKT2;1 and HvHKT2;1 were permeable to Na⁺ (see also Mian et al. (2011) for the latter transporter).

When oocytes were injected with similar amounts of *HmHKT2;1* and *HvHKT2;1* cRNA, the recorded currents were smaller in *HmHKT2;1* oocytes. Thus, we injected larger amounts of *HmHKT2;1* cRNA for compensation purpose. In the experiments analysed in Fig. 2, oocytes were injected with 50 ng of *HmHKT2;1* cRNA, against 20 ng for *HvHKT2;1*. Na⁺ transport activity has been compared in these two kinds of oocytes by using the classical Michaelis-Menten hyperbolic equation to fit the dependency of the membrane conductance (G) on Na⁺ external concentration (Fig. 2G). The K_M parameter for Na⁺ (K_M[Na⁺]) thereby obtained was 0.8 mM for HmHKT2;1 and 4.7 mM for HvHKT2;1, indicating that HmHKT2;1 displayed a much higher affinity for Na⁺ than HvHKT2;1.

Comparison of HmHKT2;1 and HvHKT2;1 K⁺ transport activity in oocytes

Experiments were carried out for the analysis of K⁺ transport activity in a similar way as described above for Na⁺ transport. Currents were recorded in oocytes bathed in solutions containing different

concentrations of K^+ , from 0.1 to 30 mM, in presence of a fixed concentration of Na^+ , 100 mM (Fig. 3). The recorded I-V curves showed that E_{rev} was shifted towards more positive membrane potentials when the external concentration of K^+ was increased (Fig. 3E, F; see also Fig. 5D). Such a shift demonstrated that both HmHKT2;1 and HvHKT2;1 were permeable to K^+ . Regarding HvHKT2;1, this conclusion is consistent with previous analyses (Mian et al. 2011).

For HvHKT2;1, analysis of the dependency of the oocyte membrane conductance on external K^+ concentration led to a K_M parameter for K^+ ($K_M[K^+]$) close to 1 mM (Fig. 3G). For HmHKT2;1, comparison of the two I-V curves obtained in presence of either 10 or 30 mM K^+ led to the conclusion that, at negative membrane potentials, the currents were smaller at the highest K^+ concentration. Such a decrease in current intensity, and thus in membrane conductance, suggested that HmHKT2;1 was blocked by high external K^+ concentrations. For an operational analysis of such a behaviour, we described the dependency of the inward conductance G on external K^+ concentration as resulting from two opposite phenomena, both described by the mass action law and Michaelis-Menten hyperbolic equation: a hyperbolic increase in the conductance with the external concentration of K^+ , characterized by a half-saturation constant K_M , and an inhibition of the conductance by the external concentration of this cation, characterized by an inhibition constant K_i (Fig. 3G). Using this formalism resulted in a K_M for K^+ ($K_M[K^+]$) close to 0.06 mM and a K_i of 216 mM. Thus, in presence of 100 mM Na^+ in the external solution, HmHKT2;1 displays a much higher affinity for K^+ than HvHKT2;1 (its $K_M[K^+]$ is lower by more than one order of magnitude) and an inhibition ("blockage") by this cation at high concentrations in the external medium. The fact that the K_i parameter describing this inhibition corresponds to a high concentration (216 mM) reflects that the blockage by K^+ was rather weak in these experimental conditions, in the presence of 100 mM Na^+ .

Comparison of the sensitivity of HmHKT2;1 and HvHKT2;1 to high K^+ concentrations

The sensitivity of HmHKT2;1 and HvHKT2;1 to high external K^+ concentrations was further compared by carrying out similar experiments as those described in the above paragraph but at lower Na^+ external concentrations, either 30 or 0.5 mM, the external concentration of K^+ being again varied between 0.03 and 30 mM. The I-V curves obtained at the different external K^+ concentrations in

presence of either 30 mM or 0.5 mM Na⁺ are displayed in Supplementary Fig. S2 and S3, respectively. Determined from these I-V curves, the changes in the oocyte membrane conductance G with the external concentration of K⁺ are displayed in Fig. 4A and 4B for the experiments carried out in presence of either 30 mM or 0.5 mM Na⁺, respectively. Analysis of these kinetics revealed that decreasing the external concentration of Na⁺ rendered the sensitivity of HmHKT2;1 to high external K⁺ concentrations stronger, when compared with that observed previously in presence of 100 mM Na⁺ (Fig. 3G; Supplementary Table S1). It also revealed that HvHKT2;1 was very strongly blocked by K⁺ in such conditions. Comparison of the kinetics observed for the two transporters indicated that the relative inhibition by high external K⁺ concentration was less pronounced in HmHKT2;1 than in HvHKT2;1 (Fig. 4; Supplementary Table S1).

Interaction between K⁺ and Na⁺ transports in HmHKT2;1 and HvHKT2;1

I-V curves obtained for HmHKT2;1 in solutions containing 10 mmol.l⁻¹ of either Na⁺, K⁺, Rb⁺, Cs⁺ or Li⁺ (Supplementary Fig. S4) showed that, amongst these monovalent cations, HmHKT2;1 is preferentially permeable to Na⁺ and K⁺, as previously shown for HvHKT2;1 (Mian et al. 2011).

Theoretical analysis (Nernst equation) indicates that the reversal potential E_{rev} of a transport system strictly permeable to a single ion, X⁺, is shifted by ca. 60 mV upon a 10-fold change in X⁺ external activity. Fig. 5 displays, for both HmHKT2;1 and HvHKT2;1, the dependency of E_{rev} (obtained from the above described I-V curves) on the external activity of either Na⁺ or K⁺, the concentration of one of these two cations being kept constant and the other one being varied. In different external conditions, within very large ranges of ion activities, the slopes of these experimental curves are close to 30 mV per decade of activity. Such a relationship can be taken as evidence that HKT transporters of this type (belonging to the HKT subfamily 2) behave as Na⁺-K⁺ symporters with a Na⁺:K⁺ stoichiometry close to 1:1 (Rubio et al. 1995, Jabnourne et al. 2009). Assuming that the Na⁺-K⁺ symport stoichiometry can vary, depending on external concentrations of K⁺ and Na⁺ (Rubio et al. 1995, Sassi et al. 2012), the proposed symport model can also account for the fact that the slope of E_{rev} curves can be much lower than 30 mV per decade of activity in some concentration conditions. It is interesting to note that while the E_{rev} curves corresponding to HmHKT2;1 and HvHKT2;1 are almost

parallel (i.e., they display the same slope) in most conditions, indicating that the Na⁺-K⁺ symport stoichiometry was the same in both transporters, they diverge when the external concentration of Na⁺ was fixed at a high value (30 or 100 mM) and the external concentration of K⁺ was varied in the low concentration range (0.1 to 1 mM) (Fig. 5C and D). In these latter conditions, the slope of the HmHKT2;1 curve becomes much smaller than that of the HvHKT2;1 curve. Within the framework of the above discussed Na⁺-K⁺ symport model, this indicates that the Na⁺:K⁺ stoichiometry, i.e., the number of Na⁺ ions transported per transported K⁺ ion, was significantly higher in HmHKT2;1 than in HvHKT2;1 in these conditions.

Molecular bases of differences in Na⁺ and K⁺ transport properties between HmHKT2;1 and HvHKT2;1

The molecular bases of observed differences in Na⁺ and K⁺ transport features between HmHKT2;1 and HvHKT2;1 were examined by domain swapping experiments between the two HKT2;1 transporters. Two chimeras, named *HvHm-5S* and *HvHm-8S*, were produced, focusing on two regions gathering two thirds of the amino acid sequence differences between the two transporters. In *HvHm-5S*, the exchanged DNA fragment resulted in the introduction in HvHKT2;1 of 6 amino acids specific to HmHKT2;1, 4 of them in the 5th transmembrane segment and 2 at the beginning of the following pore-forming region (positions 320 to 356; Fig. 1A and 6A). In *HvHm-8S*, the exchanged DNA fragment resulted in the introduction in HvHKT2;1 of 5 amino acids specific to HmHKT2;1, 2 of them in the 8th transmembrane segment and the 3 other ones at the end of the preceding pore-forming region (positions 470 to 525; Fig. 1A and 6A). The two chimeras being constituted mainly of HvHKT2;1 sequence, their functional properties were analysed in *Xenopus* oocytes injected with 20 ng of cRNA, like for HvHKT2;1 analysis (Supplementary Fig. S5 and S6).

In a first set of experiments, the apparent affinity for Na⁺ transport was compared in the HvHm-5S and HvHm-8S transporters using the set of solutions containing 0.5 mM K⁺ and varying Na⁺ concentrations (0.1 to 30 mM) like for the Na⁺ transport analyses previously performed in HmHKT2;1 and HvHKT2;1. Recorded currents indicated that the two chimeras were well expressed in oocytes and kept a large permeability to Na⁺ (Supplementary Fig. S5), as expected. Sharp differences,

however, were noticed between the two chimeras in the inward conductance saturation upon increase in the external Na⁺ concentration (Fig 6B, Supplementary Fig. S5;): HvHm-5S displayed a ~4-fold higher apparent affinity ($K_M = 0.8$ mM) than HvHm-8S ($K_M = 3$ mM). Thus, the K_M for Na⁺ transport of HvHm-5S was identical to that observed for the *H. maritimum* HKT2;1 transporter in the same conditions (Supplementary Tables S1 and S2), while that of the other chimera was close to that observed for the barley HKT2;1 transporter ($K_M = 4.7$ mM, Supplementary Tables S1 and S2). On the other hand, the maximal conductances derived from the Michaelis-Menten fits were identical for the two chimeras ($G_{max} \sim 90$ μ S), in between those of HmHKT2;1 and HvHKT2;1 (when analysed with the same level of injected cRNA).

The K⁺ transport properties of the two chimeras were also compared using one of the sets of solutions with fixed Na⁺ concentration and varying K⁺ concentrations used for the detailed analysis of HmHKT2;1 and HvHKT2;1 current sensitivity to K⁺: Na⁺ concentration was 30 mM in all solutions and K⁺ concentration varied from 0.3 mM to 30 mM. The two chimeras were shown to be largely permeable to K⁺, and to display a K⁺-induced inhibition of currents at high external K⁺ concentrations (Supplementary Fig. S6), like the *H. maritimum* and barley HKT2;1 transporters. The two chimeras, however, differed in their sensitivity to external K⁺: HvHm-5S showed a 10-fold lower inhibition of currents at high K⁺ concentration than HvHm-8S (inward conductance inhibition constant $K_i = 104$ and 11 mM, in HvHm-5S and HvHm-8S, respectively; Fig. 6C). This difference was reminiscent of that observed between *H. maritimum* and barley HKT2;1 transporters: K_i of conductance inhibition by external K⁺ 4.3-fold lower in the *H. maritimum* transporter than in the barley one (Supplementary Tables S1 and S2). On the other hand, the apparent affinity for K⁺ transport and the maximal conductance, derived from the Michaelis-Menten fits, were similar in the two chimeras ($K_M = 0.4$ and 0.3 mM in HvHm-5S and HvHm-8S, $G_{max} \sim 200$ μ S in both transporters; Fig. 6C), in between those of HmHKT2;1 and HvHKT2;1 (Fig. 4A, Fig. 6C, Supplementary Tables S1 and S2).

As a whole, the characterization of the chimeras thus indicated that the region comprised between position 320 and 356 in the *Hordeum* HKT2;1 transporters, is a strong determinant of the affinity for Na⁺ and the sensitivity to external K⁺.

***HmHKT2;1* gene expression, K⁺ and Na⁺ accumulation and plant biomass production under saline conditions**

Soliman and Kalbia ecotypes were compared with respect to *HmHKT2;1* expression, K⁺ and Na⁺ accumulation (total content) and biomass production. The standard nutrient solution was supplemented with 200 mM NaCl for 48 h or 7 days before roots and shoots were sampled, all the plants being 5 week-old when harvested (Fig. 7A).

Q-RT-PCR experiments revealed that *HmHKT2;1* displays much higher expression in roots than in shoots, in both Soliman and Kalbia ecotypes (Fig. 7B). Addition of NaCl in the external solution resulted in a significant decrease in the level of *HmHKT2;1* transcripts in Soliman but not in Kalbia plants (Fig. 7B). The two ecotypes differed in their K⁺ accumulation capacity, which was strongly decreased in Soliman but appeared unchanged in Kalbia (Fig. 8A). Na⁺ accumulation was larger in Kalbia than in Soliman plants (Fig. 8B). Finally, root and shoot biomass measurements revealed that the NaCl treatments resulted in a significant decrease in plant growth in Soliman but not in Kalbia plants (Fig. 9). An increase in root and shoot biomass was even observed in the latter ecotype.

These data were used to assess the so-called plant K⁺ absorption efficiency (KAE), the ratio of total K⁺ accumulation (expressed on a per-plant basis) by the root biomass (dry weight) (Rabhi et al. 2007, Benzarti et al. 2014). KAE appeared to be higher in Kalbia than in Soliman plants under saline conditions (Supplementary Fig. S7).

It should be noted that *Hordeum vulgare* plants were found to display much larger biomass production than *H. maritimum* Soliman and Kalbia plants when grown in parallel experiments, and submitted to the same NaCl treatments (Supplementary Fig. S8). Comparison of the consequences of the NaCl treatments on *H. maritimum* and *H. vulgare* is thus barely relevant. It is however interesting to note that the ratio of Na⁺ to K⁺ contents in shoots at the end of the 7-day treatment in 200 mM NaCl was close to 4.3 in *H. vulgare* while it was lower than 1.5 in *H. maritimum* Soliman and Kalbia plants (n = 4 for each genotype and SE lower than 20%), which reveals a tight control of Na⁺ translocation to shoots in the halophyte *H. maritimum*.

Discussion

In our conditions, *Hordeum maritimum* biomass production was much lower than that of cultivated barley (*H. vulgare*). However, it can significantly contribute to biomass production in salt-affected biotopes (Abdelly et al. 2006). It is thus a model species, with fodder potential, for studying plants adapted to strongly saline conditions (Hafsi et al. 2010, Yousfi et al. 2010).

Aiming at characterizing Na⁺ and/or K⁺ transport systems likely to play a role in *H. maritimum* tolerance to salinity, we focused on HmHKT2;1. The *HmHKT2;1* sequences cloned in the Kalbia and Soliman ecotypes encode the same polypeptide, without any amino acid difference between the two genotypes (a single silent difference was found between the 2 nucleotide sequences). Functional properties of this polypeptide, HmHKT2;1, were compared to those of HvHKT2;1 using the oocyte expression system.

Operationally, HKT2;1-type transporters can be described as endowed with 3 types of conduction states, a Na⁺-K⁺ symport state, a Na⁺ uniport state, and a nonconductive state, which results from the inhibition of the transport activity in response to high external K⁺ concentrations, the K⁺ concentration threshold above which this inhibition is detectable and the magnitude of the inhibition depending on the external concentration of Na⁺ (Rubio et al. 1995, Gassmann et al. 1996, Jabnoue et al. 2009). In wheat, TaHKT2;1 has been shown to work as a Na⁺-K⁺ symporter when the external concentrations of Na⁺ and K⁺ were balanced, and mainly as a Na⁺-selective uniporter when the concentration of Na⁺ was much higher than that of K⁺ (Rubio et al. 1995, Gassmann et al. 1996). In the rice Nipponbare OsHKT2;1 transporter, the Na⁺-K⁺ symport mode was shown to be the dominant mode at submillimolar external Na⁺ and K⁺, the Na⁺ uniport mode to be preponderant when the external concentration of Na⁺ was within or above the millimolar range and external K⁺ was in the submillimolar range, and the nonconductive state, due to K⁺ blockage, to dominate at external K⁺ in the millimolar to 10 mM range (Jabnoue et al. 2009). Interestingly, in rice, the Na⁺ and K⁺ concentration ranges within which HKT2;1-type transporters behave as Na⁺-K⁺ symporters are broader in rather salt tolerant cultivars than in the salt sensitive Nipponbare cultivar (Oomen et al. 2012). HmHKT2;1 displays several distinctive functional properties when compared with HvHKT2;1: (i)

The affinity for Na⁺ of HmHKT2;1 is higher (lower $K_M(\text{Na}^+)$ value) than that of HvHKT2;1, by about 6 times in the presence of 0.5 mM K⁺ (Fig. 2; Supplementary Table S1); (ii) The affinity of HmHKT2;1 for K⁺ is also always higher (lower $K_M(\text{K}^+)$ values) than that of HvHKT2;1, in a large range of Na⁺ concentrations (0.5, 30 or 100 mM), and is poorly dependent on the external concentration of Na⁺ (Fig. 3; Supplementary Table S1). (iii) The conductance of both transporters appears to be blocked by high external K⁺ concentrations but the relative inhibition appears to be less pronounced in HmHKT2;1 than in HvHKT2;1 in different external conditions (Fig. 4; K_i parameters in Supplementary Table S1). The whole set of data indicates that HmHKT2;1 behaves as a Na⁺-K⁺ symporter in larger ranges of K⁺ and Na⁺ concentrations, when compared with HvHKT2;1 and the wheat and rice HKT2;1 homologs previously characterized (Rubio et al. 1995, Gassmann et al. 1996, Jabnourne et al. 2009, Oomen et al. 2012).

The fact that relatively little difference in amino acid sequence distinguished HmHKT2;1 and HvHKT2;1, and that a large proportion of the residue differences are concentrated in only two regions in the sequence (Fig. 1) led us to initiate the analysis of the molecular bases of the functional differences between the two transporters, by a domain swapping strategy. Among the 6 residues varying between *H. maritimum* and barley HKT2;1 transporters, which were exchanged in the HvHm-5S chimera, 4 varied also between *H. maritimum* HKT2;1 and wheat and *Brachypodium distachyon* homologs. In the HvHm-8S chimera, 2 of the 5 residues originating from HmHKT2;1 which differed in HvHKT2;1, also differed in both TaHKT2;1 and BdHKT2;1. Very few structure function analyses have been done on HKT transporters from the subfamily 2. Random mutagenesis in the wheat *HKT2;1* sequence and site-directed mutagenesis of conserved residues in different HKT transporters led to the identification of a few point mutations which affected Na⁺ permeability or rate of transport or inhibition by K⁺ (Rubio et al. 1995, Rubio et al. 1999; Kato et al. 2007). The positions of these mutations were different from those examined using the present chimeras. Furthermore, none of these mutations occurred naturally. Here, the analyses of chimeras between HvHKT2;1 and HmHKT2;1 identified the region comprising the 5th transmembrane domain and the adjacent P loop as a strong determinant of differences in Na⁺ and K⁺ transport properties (affinity for Na⁺ transport, inhibition by high K⁺ concentrations) existing between these HKT2;1-type transporters.

K⁺ homeostasis has to be preserved in the symplasm for plant tolerance to salinity (Yeo 1983, Munns and Tester 2008, Kronzucker and Britto 2011). This requires that roots have the ability to selectively take up K⁺ even in presence of high Na⁺ concentrations. Specific functional features of HmHKT2;1, when compared with HvHKT2;1 and the OsHKT2;1 and TaHKT2;1 homologs characterized in rice and wheat, could contribute to efficient K⁺ uptake in presence of high Na⁺ concentrations, and thereby to adaptation of *H. maritimum* to high salinity conditions. The fact that the apparent K_M for K⁺ K_M(K⁺) of HmHKT2;1 remained low, below 60 μM whatever the external concentration of Na⁺ (Supplementary Table S1), even in presence of 100 mM Na⁺, could allow cells to efficiently take up K⁺ even in presence of high external concentrations of Na⁺. Also, the fact that HmHKT2;1 behaves as a symporter with a Na⁺:K⁺ stoichiometry higher than 1 Na⁺ per K⁺ in presence of low K⁺ concentrations could contribute to efficient energization of active K⁺ uptake in such conditions.

The Soliman ecotype has been extensively characterized as salt tolerant (Hafsi et al. 2010, Yousfi et al. 2010, Zribi et al. 2012). The saline treatments we used did not result in any salt-toxicity symptom detectable by eye. They however severely reduced shoot and root biomass production in the Soliman plants. This result, which is consistent with previous analyses (Hafsi et al. 2007), provides evidence that the plants suffered from the imposed saline conditions. Kalbia displayed a slightly slower growth rate than Soliman in the absence of added NaCl in the external solution but its growth was not reduced by the saline treatments we used. Thus, the Kalbia ecotype appears to be even more tolerant than Soliman, as this could be expected from the difference in salinity levels of their natural habitats (see Introduction).

Plant K⁺ absorption efficiency was reduced upon salt stress in both Kalbia and Soliman plants, but the reduction was less pronounced in Kalbia, which then displayed higher K⁺ absorption efficiency than Soliman. These two ecotypes express the same HKT2;1 transporter but differ in the regulation of the encoding gene, the transcript level decreasing in response to the saline treatments in Soliman but remaining constant in Kalbia. This may explain that K⁺ absorption efficiency was higher in Kalbia, a hypothesis which is also related to the fact that overexpression of *HvHKT2;1* in barley results in increased salt tolerance (Mian et al. 2011). It is worth to note that a counterpart of the preservation of

HmHKT2;1 expression in Kalbia under saline conditions could be the larger net uptake of Na⁺ in this ecotype than in Soliman (Fig. 8B). Functional properties and regulation of HKT transporters could reflect the need for the plant to cope with the three following objectives: to energize selective K⁺ transport in presence of high Na⁺ concentrations (Rubio et al. 1995, Ardie et al. 2009), to contribute to Na⁺ entry, allowing the use of this cation for osmotic adjustment (Yeo 1983, Horie et al. 2007, Flowers and Colmer 2008), and to prevent excessive Na⁺ transport and accumulation in plant tissues. It is tempting to speculate that the regulation of *HmHKT2;1* expression in response to external salinity and especially the control of the activity of the encoded transporter by external K⁺ contribute to the integration of these three objectives and plant adaptation to high salinity levels.

Materials and Methods

Plant material and growth conditions

H. maritimum seeds were collected from Soliman (30 Km south of Tunis) and Kalbia (in center of Tunisia) sebkhas. Seeds of *H. vulgare* (var. Manel) were obtained from the National Institute of Agronomic Research of Tunis. Seeds were disinfected with sodium hypochlorite (1%) for a few minutes and thoroughly rinsed with distilled water. They were then germinated in Petri dishes. After one week, the seedlings were transferred onto hydroponic medium (Fig. 7A) in plastic tubs (8 liters) filled with modified Hewitt's nutrient solution (Hewitt 1966) and placed in a growth chamber set to a light/dark cycle of 16h/8h (photosynthetically active radiation 300 $\mu\text{mol m}^{-2} \text{s}^{-1}$), 20-24°C day/night, and 40 to 60% relative humidity. The nutrient solution contained the following macronutrients (in mM): MgSO₄ (1.5), KH₂PO₄ (1.6), NH₄NO₃ (2), Ca(NO₃)₂ (5) and Na₂HPO₄ (0.4). The micronutrients were (in μM): Mn (9), Cu (0.6), Zn (0.7), B (4.6), Mo (0.2) (Arnon and Hoagland 1940) and Fe (53) (Jacobson 1951). The solution was renewed every 3 days. Plants grown in such conditions for 5 weeks were used as control. Other plants, grown in parallel, were submitted to NaCl treatments: the hydroponic solution was supplemented with 200 mM NaCl either 48 h or 7 days before the end of the 5th week of

growth. Thus, control and salt-treated plants were harvested exactly at the same time, after 5 weeks of growth in hydroponic conditions.

Biomass and ion content analyses

Shoot and root dry weights (DW) were measured after 72 h at 60 °C. Sodium and potassium contents were assayed by flame spectrophotometry after extraction from dry tissues with 0.1 N HCl. Potassium Absorption Efficiency (KAE, in $\mu\text{mol K}^+/\text{mg DW}$ roots) was determined as the ratio of the total (root + shoot) plant K^+ content divided by the root dry weight.

Isolation of *Hordeum maritimum* *HmHKT2;1* cDNA

RNA from 18-day-old *H. maritimum* Soliman and Kalbia seedlings was extracted using RNeasy Mini Kit (Qiagen). To remove contaminating genomic DNA, total RNA (2.5 μg) was treated with DNase using DNase I Kit (Invitrogen). DNase-treated RNA (1 μg) was reverse transcribed using a ThermoScientific Revert Aid Premium Reverse Transcriptase (200 U/ μl). Two microliters of first-strand cDNA was used as template for PCR amplification of *HmHKT2;1* sequence using iProof High-Fidelity DNA polymerase in a reaction solution prepared according to the instructions of the manufacturer (BIO-RAD). Primers, designed on the basis of alignment of *HKT2;1*-type sequences from different Poaceae, hybridizing on 5'-UTR and 3'-UTR sequences, were 5'-TCGCACTCATATATAGCACCATG-3' (Forward) and 5'-CCAAGTAATCTTGGTCACTTGTATCA-3' (Reverse). Amplified products were treated for 15 min at 72°C in the presence of GoTag polymerase and dATP, for desoxyadenosine addition at the 3' end, then cloned in the pGEM-T Easy vector (Promega) and sequenced.

Quantitative RT-PCR analyses

DNase-treated RNA samples (1.5 μg) from total RNA extracted using RNeasy Mini Kit (Qiagen) were used to synthesize first-strand cDNA using the SuperScript III Reverse Transcriptase (200 U/ μl) (Invitrogen). Primer pairs were designed from *HmHKT2;1* and reference gene coding sequences (*actin*

and *EF1*) using Primer3 software with the following parameters: T_m between 59 and 61 °C; PCR product size of 103-138 base pairs (bp); primer length of 18-20 bp, and GC content of 50-55%. *HmHKT2;1* specific primers: 5'-CTCTGATGAGTCGCAGCTTG-3' (Forward) and 5'-GGCAAAGTACCCAAAGACCA-3' (Reverse); *actin*: 5'-CAATGTTCTGCCATGTACG-3' (Forward) and 5'-ATGAGGAAGGGCGTATCCTT3' (Reverse); *EF1*: 5'-TCTCTGGGTTTGAGGGTGAC-3' (Forward) and 5'-CTTGGGCTCATTGATCTGGT-3' (Reverse). First strand cDNA was used as a template for qRT-PCR. PCR were performed in 96-well blocks with a LightCycler 480 Real-Time PCR system using SYBR Green 1 Master mix (Roche), as recommended by the manufacturer: 10 min at 95°C, 45 cycles at 95°C for 10 s, 60°C for 10 s and an elongation phase of 72°C for 15 s. At the end of the reaction process, the dissociation curve was derived by heating the amplicon from 65 to 97°C (at a rate of 0.11°C/s). All qRT-PCR were run in technical and biological triplicates.

Absolute numbers of *HmHKT2;1* cDNA molecules were determined using standard curves obtained from dilution series of known amounts of fragments from the corresponding cDNA. Rough expression values of *HmHKT2;1* were slightly corrected using a normalization factor obtained by geometric averaging of *actin* and *EF1* reference gene expression values using GeNorm V.3 (Vandesompele et al. 2002).

Construction of chimeric *H. vulgare/H. maritimum HKT2;1* cDNA

Chimeric *HKT2;1* cDNA were produced using *H. maritimum* and barley *HKT2;1* cDNA subcloned into the *Xenopus* oocyte expression vector (see below) and common restriction sites for domain swapping: *BstEII* (position 709) and *NsiI* (position 1078) for the chimera *HvHm-5S*, *NdeI* (position 1399) and the *HindIII* site downstream of the cDNA in the vector cloning cassette for the chimera *HvHm-8S* (Fig 6A).

Expression in *Xenopus laevis* oocytes

. Capped and polyadenylated cRNA were synthesized *in vitro*, using the mMACHINE T7 kit (Ambion), from linearized pGEMXho vector (Mian et al. 2011) containing *H. maritimum*, barley or chimeric *HKT2;1* cDNA subcloned downstream from the T7 promoter between the 5' and 3'

untranslated regions of the *Xenopus β -globin* gene. Oocytes were isolated as described previously (Véry et al. 1995), injected with either 50 nl of DNase-free water (for control oocytes) or with 50 ng of *HmHKT2;1* or 20 ng of *HvHKT2;1*, *HvHm-5S* or *HvHm-8S* cRNA (unless otherwise stated in the Figure legends) in 50 nl DNase-free water, and then kept at 19 °C in ND96 medium (96 mM NaCl, 2 mM KCl, 1.8 mM CaCl₂, 1 mM MgCl₂, 2.5 mM Na-pyruvate, and 5 mM HEPES-NaOH, pH 7.4) supplemented with 0.5 mg.l⁻¹ gentamycin until electrophysiological recordings.

Two-Electrode Voltage Clamp

Whole-cell currents from oocytes were recorded using the two-electrode voltage clamp technique. The voltage-clamp amplifier was a GeneClamp 500B (Axon Instruments). Voltage-pulse protocols, data acquisition and data analyses were performed using Pclamp10 (Axon Instruments) and Sigmaplot 9 (Systat Software) softwares. Both applied voltage (V) and current (I) were recorded. In the resulting I/V plots, inward conductances were defined as the slopes of the I-V curve between the three most negative imposed voltages for each ionic condition. A correction was made for the voltage decrease resulting from the series resistance of the bath and the reference electrode using two external electrodes connected to a bath probe (VG-2A x100 Virtual-ground bath clamp; Axon Instruments). Electrodes were filled with 3 M KCl. Bath solutions were continuously perfused during the experiment and contained 6 mM MgCl₂, 1.8 mM CaCl₂ and 10 mM MES/bis-Tris Propane (pH 5.5). Alkaline monovalent cations (K⁺, Na⁺, Li⁺, Rb⁺ or Cs⁺) were added as glutamate or chloride salts (as indicated in the figure legends). D-mannitol was added when necessary to adjust the osmolarity in the 200-240 mOsmol.l⁻¹ range in each set of solutions. The actual K⁺ and Na⁺ concentrations of the solutions were measured by flame spectrophotometry. Currents through *HmHKT2;1*, *HvHKT2;1* and the *HvHm* chimeric transporters were calculated by subtracting from the total currents recorded in the oocytes expressing *HmHKT2;1*, *HvHKT2;1* or the *HvHm* transporters the corresponding mean currents recorded in four water injected oocytes from the same batch under the same ionic and electrical conditions.

Funding. This work was supported in part by the Tunisian Ministry of Higher Education and Scientific Research (LR15CBBC02).

Conflicts of interest: No conflicts of interest declared

Acknowledgments.

References

- Abdelly, C., Barhoumi, Z. and Ghnaya, T. (2006) Potential utilisation of halophytes for the rehabilitation and valorisation of salt-affected areas in Tunisia. *Biosaline Agriculture and Salinity Tolerance in Plants* 163–172.
- Ardie, S.W., Xie, L., Takahashi, R., Liu, S. and Takano, T. (2009) Cloning of a high-affinity K⁺ transporter gene PutHKT2;1 from *Puccinellia tenuiflora* and its functional comparison with OsHKT2;1 from rice in yeast and *Arabidopsis*. *Journal of Experimental Botany* 60: 3491–3502.
- Anon, D.I. and Hoagland, D.R. (1940) Crop production in artificial culture solutions and in soils with special reference to factors influencing yields and absorption of inorganic nutrients. *Soil Science* 50: 463–485.
- Asins, M.J., Villalta, I., Aly, M.M., et al. (2013) Two closely linked tomato HKT coding genes are positional candidates for the major tomato QTL involved in Na⁺/K⁺ homeostasis. *Plant, Cell and Environment* 36: 1171–1191.
- Benzarti, M., Ben Rejeb, K., Messedi, D., Ben Mna, A., Hessini, K., Ksontini, M., et al. (2014) Effect of high salinity on *Atriplex portulacoides*: Growth, leaf water relations and solute accumulation in relation with osmotic adjustment. *South African Journal of Botany* 95: 70–77.
- Berthomieu, P., Conéjéro, G., Nublat, A., et al. (2003) Functional analysis of AtHKT1 in *Arabidopsis* shows that Na⁺ recirculation by the phloem is crucial for salt tolerance. *EMBO Journal* 22: 2004–2014.
- Byrt, C.S., Platten, J.D., Spielmeyer, W., James, R.A., Lagudah, E.S., Dennis, E.S., et al. (2007) HKT1; 5-like cation transporters linked to Na⁺ exclusion loci in wheat, Nax2 and Kna1. *Plant Physiology* 143: 1918–1928.
- Campbell, M.T., Bandillo, N., Al Shiblawi, F.R.A., et al. (2017) Allelic variants of OsHKT1;1 underlie the divergence between indica and japonica subspecies of rice (*Oryza sativa*) for root sodium content. *PLoS Genetics* 13: e1006823.
- Chen, H., An, R., Tang, J.H., Cui, X.H., Hao, F.S., Chen, J. and Wang, X.C. (2007) Over-expression of a vacuolar Na⁺/H⁺ antiporter gene improves salt tolerance in an upland rice. *Molecular Breeding* 19: 215–225.

- Corratgé-Faillie, C., Jabnourne, M., Zimmermann, S., Véry, A.-A., Fizames, C. and Sentenac, H. (2010) Potassium and sodium transport in non-animal cells: the Trk/Ktr/HKT transporter family. *Cellular and Molecular Life Sciences* 67: 2511–2532.
- Cuénod, A., Pottier-Alapetite, G. and Labre, A. (1954) Flore analytique et synoptique de Tunisie: Cryptogames vasculaires. *Gymnospermes et Monocotylédones, SEFAN, Tunis*.
- Deinlein, U., Stephan, A.B., Horie, T., Luo, W., Xu, G. and Schroeder, J.I. (2014) Plant salt-tolerance mechanisms. *Trends in Plant Science* 19: 371–379.
- Durell, S.R., Hao, Y., Nakamura, T., Bakker, E.P. and Guy, H.R. (1999) Evolutionary relationship between K⁺ channels and symporters. *Biophysical journal* 77: 775–788.
- Flowers, T.J. (1985) Physiology of halophytes. *Plant and Soil* 89: 41–56.
- Flowers, T.J. and Colmer, T.D. (2008) Salinity tolerance in halophytes. *New Phytologist* 179: 945–963.
- Gassmann, W., Rubio, F. and Schroeder, J.I. (1996) Alkali cation selectivity of the wheat root high-affinity potassium transporter HKT1. *Plant Journal* 10: 869–882.
- Gaxiola, R.A., Li, J., Undurraga, S., Dang, L.M., Allen, G.J., Alper, S.L. and Fink, G.R. (2001) Drought- and salt-tolerant plants result from overexpression of the AVP1 H⁺-pump. *Proceedings of the National Academy of Sciences of the U.S.A.* 98: 11444–11449.
- Greenway, H. and Munns, R. (1980) Mechanisms of salt tolerance in nonhalophytes. *Annual Review of Plant Physiology* 31: 149–190.
- Hachicha, M. (2007) Les sols salés et leur mise en valeur en Tunisie. *Science et changements planétaires/Sécheresse* 18: 45–50.
- Hafsi, C., Lakhdhar, A., Rabhi, M., Debez, A., Abdelly, C. and Ouerghi, Z. (2007) Interactive effects of salinity and potassium availability on growth, water status, and ionic composition of *Hordeum maritimum*. *Journal of Plant Nutrition and Soil Science* 170: 469–473.
- Hafsi, C., Romero-Puertas, M.C., Gupta, D.K., Luis, A., Sandalio, L.M. and Abdelly, C. (2010) Moderate salinity enhances the antioxidative response in the halophyte *Hordeum maritimum* L. under potassium deficiency. *Environmental and Experimental Botany* 69: 129–136.
- Hamamoto, S., Horie, T., Hauser, F., Deinlein, U., Schroeder, J.I. and Uozumi, N. (2015) HKT transporters mediate salt stress resistance in plants: From structure and function to the field.

Current Opinion in Biotechnology 32: 113–120.

- Haro, R., Bañuelos, M.A., Senn, M.E., Barrero-Gil, J. and Rodríguez-Navarro, A. (2005) HKT1 mediates sodium uniport in roots. Pitfalls in the expression of HKT1 in yeast. *Plant Physiology* 139: 1495–506.
- Hartley, T.N., Thomas, A.S., Maathuis, F.J.M. (2019) A role for the OsHKT 2;1 sodium transporter in potassium use efficiency in rice. *Journal of Experimental Botany* (doi: 10.1093/jxb/erz113).
- Hasegawa, P.M., Bressan, R.A., Zhu, J.K. and Bohnert, H.J. (2000) Plant cellular and molecular responses to high salinity. *Annual Review of Plant Biology* 51: 463–499.
- Hauser, F. and Horie, T. (2010) A conserved primary salt tolerance mechanism mediated by HKT transporters: a mechanism for sodium exclusion and maintenance of high K^+/Na^+ ratio in leaves during salinity stress. *Plant, Cell & Environment* 33: 552–565.
- Hewitt, E.J. (1966) Sand and water culture methods used in the study of plant nutrition, *Commonwealth Agricultural Bureaux*.
- Horie, T., Costa, A., Kim, T.H., et al. (2007) Rice OsHKT2;1 transporter mediates large Na^+ influx component into K^+ -starved roots for growth. *EMBO Journal* 26: 3003–3014.
- Howe, K., Bateman, A. and Durbin, R. (2002). QuickTree: building huge Neighbour-Joining trees of protein sequences. *Bioinformatics* 18(11): 1546–1547.
- Huang, S., Spielmeier, W., Lagudah, E.S., James, R.A., Platten, J.D., Dennis, E.S. and Munns, R. (2006) A sodium transporter (HKT7) is a candidate for Nax1, a gene for salt tolerance in durum wheat. *Plant Physiology* 142: 1718–1727.
- Jabnourne, M., Espeout, S., Mieulet, D., et al. (2009) Diversity in expression patterns and functional properties in the rice HKT transporter family. *Plant Physiology* 150: 1955–1971.
- Jacobson, L. (1951) Maintenance of iron supply in nutrient solutions by a single addition of ferric potassium ethylenediamine tetra-acetate. *Plant Physiology* 26: 411.
- James, R.A., Blake, C., Byrt, C.S. and Munns, R. (2011) Major genes for Na^+ exclusion, Nax1 and Nax2 (wheat HKT1;4 and HKT1;5), decrease Na^+ accumulation in bread wheat leaves under saline and water logged conditions. *Journal of Experimental Botany* 62: 2939–2947.
- Kato, N., Akai, M., Zulkifli, L., Matsuda, N., Kato, Y., Goshima, S., Hazama, A., Yamagami, M., Guy,

- H.R., Uozumi, N. (2007) Role of positively charged amino acids in the M2D transmembrane helix of Ktr/Trk/HKT type cation transporters. *Channels* 1: 161–171.
- Kato, Y., Sakaguchi, M., Mori, Y., Saito, K., Nakamura, T., Bakker, E.P., et al. (2001) Evidence in support of a four transmembrane-pore-transmembrane topology model for the *Arabidopsis thaliana* Na⁺/K⁺ translocating AtHKT1 protein, a member of the superfamily of K⁺ transporters. *Proceedings of the National Academy of Sciences of the U.S.A.* 98: 6488–6493.
- Kronzucker, H.J. and Britto, D.T. (2011) Sodium transport in plants: a critical review. *New Phytologist* 189: 54–81.
- Mian, A., Oomen, R.J.F.J., Isayenkov, S., Sentenac, H., Maathuis, F.J.M. and Véry, A.A. (2011) Over-expression of an Na⁺- and K⁺-permeable HKT transporter in barley improves salt tolerance. *Plant Journal* 68: 468–479.
- Mitsuya, S., Taniguchi, M., Miyake, H. and Takabe, T. (2005) Disruption of RCI2A leads to over-accumulation of Na⁺ and increased salt sensitivity in *Arabidopsis thaliana* plants. *Planta* 222: 1001–1009.
- Morant-Manceau, A., Pradier, E. and Tremblin, G. (2004) Osmotic adjustment, gas exchanges and chlorophyll fluorescence of a hexaploid triticale and its parental species under salt stress. *Journal of Plant Physiology* 161: 25–33.
- Munns, R. and Tester, M. (2008) Mechanisms of salinity tolerance. *Annual Review of Plant Biology* 59: 651–81.
- Nieves-Cordones, M., Alemán, F., Martínez, V. and Rubio, F. (2010) The *Arabidopsis thaliana* HAK5 K⁺ transporter is required for plant growth and K⁺ acquisition from low K⁺ solutions under saline conditions. *Molecular Plant* 3: 326–333.
- Nieves-Cordones, M., Martínez, V., Benito, B. and Rubio, F. (2016) Comparison between *Arabidopsis* and rice for main pathways of K⁺ and Na⁺ uptake by roots. *Frontiers in Plant Science* 7: 992.
- Niu, X., Bressan, R.A., Hasegawa, P.M. and Pardo, J.M. (1995) Ion Homeostasis in NaCl Stress Environments. *Plant Physiology* 109: 735–742.
- Oomen, R.J.F.J., Benito, B., Sentenac, H., Rodríguez-Navarro, A., Talón, M., Véry, A.-A. and Domingo, C. (2012) HKT2;2/1, a K⁺-permeable transporter identified in a salt-tolerant rice cultivar

- through surveys of natural genetic polymorphism. *Plant Journal* 71: 750–762.
- Platten, J.D., Cotsaftis, O., Berthomieu, P., et al. (2006) Nomenclature for HKT transporters, key determinants of plant salinity tolerance. *Trends in Plant Science* 11: 372–374.
- Rabhi, M., Barhoumi, Z., Ksouri, R., Abdelly, C. and Gharsalli, M. (2007) Interactive effects of salinity and iron deficiency in *Medicago ciliaris*. *Comptes rendus biologiques* 330: 779–788.
- Rabhi, M., Hafsi, C., Lakhdar, A., Hajji, S., Barhoumi, Z., Hamrouni, M.H., et al. (2009) Evaluation of the capacity of three halophytes to desalinize their rhizosphere as grown on saline soils under nonleaching conditions. *African Journal of Ecology* 47: 463–468.
- Ren, X., Qi, G., Feng, H., Zhao, S., Zhao, S., Wang, Y. and Wu, W. (2013) Calcineurin B-like protein CBL10 directly interacts with AKT1 and modulates K⁺ homeostasis in *Arabidopsis*. *Plant Journal* 74: 258–266.
- Ren, Z.H., Gao, J.P., Li, L.G., et al. (2005) A rice quantitative trait locus for salt tolerance encodes a sodium transporter. *Nature Genetics* 37: 1141–1146.
- Rubio, F., Gassmann, W. and Schroeder, J.I. (1995) Sodium-driven potassium uptake by the plant potassium transporter HKT1 and mutations conferring salt tolerance. *Science* 270: 1660–1663.
- Rubio, F., Schwarz, M., Gassmann, W., Schroeder, J.I. (1999) Genetic selection of mutations in the high affinity K⁺ transporter HKT1 that define functions of a loop site for reduced Na⁺ permeability and increased Na⁺ tolerance. *Journal of Biological Chemistry* 274: 6839–6847.
- Saadia, M., Jamil, A., Ashraf, M. and Akram, N.A. (2013) Comparative study of SOS2 and a novel PMP3-1 gene expression in two sunflower (*Helianthus annuus* L.) lines differing in salt tolerance. *Applied Biochemistry and Biotechnology* 170: 980–987.
- Sassi, A., Mieulet, D., Khan, I., Moreau, B., Gaillard, I., Sentenac, H. and Véry, A.-A. (2012) The Rice Monovalent Cation Transporter OsHKT2;4: Revisited Ionic Selectivity. *Plant Physiology* 160: 498–510.
- Shi, H., Ishitani, M., Kim, C. and Zhu, J.K. (2000) The *Arabidopsis thaliana* salt tolerance gene SOS1 encodes a putative Na⁺/H⁺ antiporter. *Proceedings of the National Academy of Sciences of the U.S.A.* 97: 6896–6901.
- Shi, H., Lee, B., Wu, S.J. and Zhu, J.K. (2003) Overexpression of a plasma membrane Na⁺/H⁺

- antiporter gene improves salt tolerance in *Arabidopsis thaliana*. *Nature Biotechnology* 21: 81.
- Singh, V.K., Singh, B.D., Kumar, A., Maurya, S., Krishnan, S.G., Vinod, K.K., Singh, M.P., Ellur, R.K., Bhowmick P.K. and Singh, A.K. (2018) Marker-Assisted Introgression of Saltol QTL enhances seedling stage salt tolerance in the rice variety "Pusa Basmati 1". *Hindawi International Journal of Genomics* 2018: 8319879.
- Suzuki, K., Yamaji, N., Costa, A., et al. (2016) OsHKT1; 4-mediated Na⁺ transport in stems contributes to Na⁺ exclusion from leaf blades of rice at the reproductive growth stage upon salt stress. *BMC Plant Biology* 16: 22.
- Tamura, K., Stecher, G., Peterson D., Filipinski A. and Kumar S. (2013) MEGA6: Molecular Evolutionary Genetics Analysis Version 6.0. *Molecular Biology and Evolution* 30: 2725-2729.
- Thomson, M.J., de Ocampo, M., Egdane, J., Akhlaqur Rahman, M., Godwin Sajise, A., Adorada, D.L., Tumimbang-Raiz, E., Blumwald E., Seraj, Z.I., Singh, R.K., Gregorio, G.B. and Ismail, A.M. (2010) Characterizing the Saltol Quantitative Trait Locus for salinity tolerance in rice. *Rice* 3: 148–160.
- Vandesompele, J., De Preter, K., Pattyn, F., Poppe, B., Van Roy, N., De Paepe, A. and Speleman, F. (2002) Accurate normalization of real-time quantitative RT-PCR data by geometric averaging of multiple internal control genes. *Genome Biology* 3: research0034–1.
- Véry, A.-A., Gaymard, F., Bosseux, C., Sentenac, H. and Thibaud, J.-B (1995) Expression of a cloned plant K⁺ channel in *Xenopus* oocytes: analysis of macroscopic currents. *Plant Journal* 7: 321–332.
- Véry, A.-A., Nieves-Cordones, M., Daly, M., Khan, I., Fizames, C. and Sentenac, H. (2014) Molecular biology of K⁺ transport across the plant cell membrane: what do we learn from comparison between plant species? *Journal of Plant Physiology* 171: 748–769.
- Yeo, A.R. (1983) Salinity resistance: Physiologies and prices. *Physiologia Plantarum* 58: 214–222.
- Yokoi, S., Quintero, F.J., Cubero, B., Ruiz, M.T., Bressan, R.A., Hasegawa, P.M. and Pardo, J.M. (2002) Differential expression and function of *Arabidopsis thaliana* NHX Na⁺/H⁺ antiporters in the salt stress response. *Plant Journal* 30: 529–539.
- Yousfi, S., Rabhi, M., Hessini, K., Abdelly, C. and Gharsalli, M. (2010) Differences in efficient

metabolite management and nutrient metabolic regulation between wild and cultivated barley grown at high salinity. *Plant Biology* 12: 650–658.

Zhao, F.Y., Zhang, X.J., Li, P.H., Zhao, Y.X. and Zhang, H. (2006) Co-expression of the *Suaeda salsa* SsNHX1 and *Arabidopsis* AVP1 confer greater salt tolerance to transgenic rice than the single SsNHX1. *Molecular Breeding* 17: 341–353.

Zribi, O.T., Labidi, N., Slama, I., Debez, A., Ksouri, R., Rabhi, M., et al. (2012) Alleviation of phosphorus deficiency stress by moderate salinity in the halophyte *Hordeum maritimum* L. *Plant Growth Regulation* 66: 75–85.

Figure legends

Fig. 1. Analysis of HmHKT2;1 sequence.

(A) Topology of HKT transporters and localization of the differences in amino acids between HmHKT2;1 and HvHKT2;1. HKT polypeptides are characterized by a hydrophobic core comprised of 4 MPM (for transMembrane-Pore-transMembrane) domains, and short N-and C-terminal cytosolic tails. Stars and the corresponding numbers indicate the relative position of the amino acid differences between HmHKT2;1 and HvHKT2;1.

(b) List of the differences in amino acids between HmHKT2;1 and HvHKT2;1.

(c) Phylogenetic relationships between HKT transporters from rice, wheat and barley. The unrooted phylogenetic tree was constructed from full polypeptide sequences aligned with MEGA6 (Tamura et al. 2013) with the neighbor-joining method with 10000 bootstrap replicates, using QuickTree software (Howe et al. 2002). Bootstrap values (as percentages) are indicated at the corresponding nodes. The protein accession numbers are: OsHKT1;3, CAD37185; OsHKT1;5, BAB93392; OsHKT1;4, CAD37197; OsHKT1;1, CAD37183; OsHKT2;3, CAD37187, OsHKT2;4, CAD37199; OsHKT2;1, BAB61789; OsHKT2;2, BAB61791; HvHKT2;1, CAJ01326; HmHKT2;1, MH019217; TaHKT2;1, AAA52749. *Os*, *Oryza sativa*; *Ta*, *Triticum aestivum*; *Hv*, *Hordeum vulgare*.

Fig. 2. HmHKT2;1 Na⁺ transport activity and inward conductance in *Xenopus* oocytes. Currents were recorded in solutions containing a fixed concentration of K⁺ (0.5 mM) and different concentrations of Na⁺ (0.03 to 30 mM).

(A) Voltage-clamp protocol.

(B) Representative current traces recorded in control oocytes (injected with water) bathed in 0.5 mM K⁺ background solution supplemented with 30 mM Na⁺ (30Na-0.5K solution).

(C) Representative current traces recorded in oocytes injected with 50 ng HmHKT2;1 and bathed in 30Na-0.5K solution.

(D) Representative current traces recorded in oocytes injected with 20 ng HvHKT2;1 and bathed in 30Na-0.5K solution.

(E, F) HmHKT2;1 and HvHKT2;1 current-voltage (I/V) curves at different Na^+ external concentrations.

(G) HmHKT2;1 and HvHKT2;1 inward conductance dependency on external Na^+ concentration. Inward conductances were defined as the slopes of I-V relationships between the three most negative imposed potentials for each ionic condition. The conductance was extracted from I-V data shown in panel (E) and (F) for HmHKT2;1 and HvHKT2;1, respectively. The data were fitted (solid line) with a Michaelis–Menten equation to determine the apparent half-saturation constant (K_M) using the following equation: $G = G_{\text{max}} \times [\text{Na}^+]/(K_M + [\text{Na}^+])$. Fit parameters for HmHKT2;1: $K_M = 0.8$ mM and $G_{\text{max}} = 94$ μS . For HvHKT2;1: $K_M = 4.7$ mM and $G_{\text{max}} = 280$ μS . Means \pm SE; $n = 6$ and $n = 4$ for HmHKT2;1 and HvHKT2;1, respectively.

Fig. 3. HmHKT2;1 K^+ transport activity and inward conductance in *Xenopus* oocytes in presence of 100 mM Na^+ . Currents were recorded in solutions containing a fixed concentration of Na^+ (100 mM) and different concentrations of K^+ (0.03 to 30 mM).

(A) Voltage-clamp protocol.

(B) Representative current traces recorded in control oocytes (injected with water) bathed in the 100 mM Na^+ background solution supplemented with 30 mM K^+ (100Na-30k solution).

(C) Representative current traces recorded in oocytes expressing HmHKT2;1 and bathed in 100Na-30K solution.

(D) Representative current traces recorded in oocytes expressing HvHKT2;1 and bathed in 100Na-30K solution.

(E, F) HmHKT2;1 and HvHKT2;1 current-voltage (I/V) curves at different K^+ external concentrations. Inset: I/V relationships obtained with 10 and 30 mM K^+ only.

(G) HmHKT2;1 and HvHKT2;1 inward conductance dependency on external K^+ concentration. Inward conductances were defined as the slopes of I-V relationships between the three most negative imposed potentials for each ionic condition. The conductance was extracted from I-V data shown in panels E and F for HmHKT2;1 and HvHKT2;1, respectively. For HvHKT2;1, the data were fitted (dotted line) with a Michaelis–Menten equation to determine the apparent half-saturation constant for K^+ (K_M) using the equation: $G = G_{\text{max}} \times [\text{K}^+]/(K_M + [\text{K}^+])$. Fit parameters: $K_M = 1$ mM and $G_{\text{max}} = 205$

μS . For HmHKT2;1, the results provide evidence of a decrease in inward conductance at high K^+ concentrations since the I/V curve at 30 mM K^+ crosses the curve at 10 mM K^+ and displays a slope (at the most negative membrane potentials) smaller than that of the latter I/V curve (at 10 mM K^+). In order to take into account such an inhibiting effect of high K^+ concentrations on HmHKT2;1 inward conductance, the kinetics data were fitted (solid lines) using the equation: $G = G_{\text{max}} \times \left\{ \frac{[\text{K}^+]}{K_{\text{M}} + [\text{K}^+]} \right\} \left\{ 1 - \frac{[\text{K}^+]}{K_{\text{i}} + [\text{K}^+]} \right\}$, which describes the dependency of the inward conductance on external K^+ concentration as resulting from two opposite phenomena: a hyperbolic increase in the conductance with the external concentration of K^+ , $\left\{ \frac{[\text{K}^+]}{K_{\text{M}} + [\text{K}^+]} \right\}$, characterized by a half-saturation constant K_{M} , and an inhibition of the conductance by the external concentration of this cation, $\left\{ 1 - \frac{[\text{K}^+]}{K_{\text{i}} + [\text{K}^+]} \right\}$, characterized by an inhibition constant K_{i} . Fit parameters: $K_{\text{M}} = 0.06 \text{ mM}$, $K_{\text{i}} = 216 \text{ mM}$ and $G_{\text{max}} = 101 \mu\text{S}$. Means \pm SE; $n = 4$.

Fig. 4. Inhibition of HmHKT2;1 and HvHKT2;1 conductance by increased external K^+ concentrations in presence of 30 mM or 0.5 mM Na^+ . Currents were recorded in solutions containing a fixed concentration of Na^+ (30 mM or 0.5 mM) and different concentrations of K^+ (0.03 to 30 mM), the corresponding current-voltage (I/V) curves being shown in Supplementary Fig. S3. The methodology to investigate the dependency of the transporter inward conductance on external K^+ concentration by using such I/V curves is described in the legend to Fig. 3, the experimental data being fitted (solid lines) with the equation $G = G_{\text{max}} \left\{ \frac{[\text{K}^+]}{K_{\text{M}} + [\text{K}^+]} \right\} \left\{ 1 - \frac{[\text{K}^+]}{K_{\text{i}} + [\text{K}^+]} \right\}$.

(A) Kinetics in presence of 30 mM Na^+ . Fit parameters: $K_{\text{M}} = 0.05 \text{ mM}$, $K_{\text{i}} = 24 \text{ mM}$ and $G_{\text{max}} = 93 \mu\text{S}$ for HmHKT2;1, and $K_{\text{M}} = 1.3 \text{ mM}$, $K_{\text{i}} = 5.6 \text{ mM}$ and $G_{\text{max}} = 601 \mu\text{S}$ for HvHKT2;1.

(B) Kinetics in presence of 0.5 mM Na^+ . Fit parameters: $K_{\text{M}} = 0.02 \text{ mM}$, $K_{\text{i}} = 9 \text{ mM}$ and $G_{\text{max}} = 22.4 \mu\text{S}$ for HmHKT2;1, and $K_{\text{M}} = 0.04 \text{ mM}$, $K_{\text{i}} = 4.9 \text{ mM}$ and $G_{\text{max}} = 110 \mu\text{S}$ for HvHKT2;1. Means \pm SE. Analysis in presence of 30 mM Na^+ : $n = 5$. Analysis in presence of 0.5 mM Na^+ : $n = 3$ and $n = 4$ for HmHKT2;1 and HvHKT2;1, respectively.

Fig. 5. Sensitivity of HmHKT2;1 and HvHKT2;1 zero current potential (Erev) to external Na^+ or K^+ activity. (A) 0.5 mM K^+ , Na^+ concentration varied. (B) 0.5 mM Na^+ , K^+ concentration varied. (C) 30 mM

Na⁺, K⁺ concentration varied. (D) 100 mM Na⁺, K⁺ concentration varied. Data are taken from the experiments shown in Fig. 2E and F for panel A, from Supplementary Fig. S3 for panel B, from Supplementary Fig. S2 for panel C, and from Fig. 3E and F for panel D. Means \pm SE; $n \geq 3$ (see the legends of the corresponding figures).

Fig. 6. Inward conductance dependency on external Na⁺ and K⁺ concentrations in the chimeric transporters HvHm-5S and HvHm-8S.

(A) Topology of the chimeric transporters showing the regions from *H. maritimum* introduced in *H. vulgare*. *H. vulgare* regions are in dark grey. The region originating from *H. maritimum* is in pale gray. In the latter region, the stars indicate the positions of amino acids specific to *H. maritimum*.

(B) Inward conductance dependency on external Na⁺ concentration. *Xenopus* oocytes were injected with 20 ng of *HvHm-5S* or *HvHm-8S* cRNA. Currents were recorded in solutions containing 0.5 mM K⁺ and different concentrations of Na⁺ (0.1 to 30 mM), the corresponding I/V curves being shown in Supplementary Fig. S5. Inward conductances were determined from I/V relationships and fitted to a Michaelis–Menten equation as described in the legend to Fig. 2G. Fit parameters: for HvHm-5S, $K_M = 0.8$ mM and $G_{max} = 87$ μ S, for HvHm-8S, $K_M = 3$ mM and $G_{max} = 88$ μ S.

(C) Inward conductance dependency on external K⁺ concentration. *Xenopus* oocytes were injected with 20 ng of *HvHm-5S* or *HvHm-8S* cRNA. Currents were recorded in solutions containing 30 mM Na⁺ and different concentrations of K⁺ (0.3 to 30 mM), the corresponding I/V curves being shown in Supplementary Fig. S6. Inward conductances were determined from I/V relationships and fitted to the equation $G = G_{max} \{ [K^+]/(K_M + [K^+]) \} \{ 1 - [K^+]/(K_i + [K^+]) \}$, as described in the legend to Fig. 4. Fit parameters: for HvHm-5S, $K_M = 0.4$ mM, $K_i = 104$ mM and $G_{max} = 207$ μ S, for HvHm-8S, $K_M = 0.3$ mM, $K_i = 11$ mM and $G_{max} = 175$ μ S.

Fig. 7. *HmHKT2;1* transcript accumulation in shoots and roots of *Hordeum maritimum* Kalbia and Soliman plants grown in standard solution or submitted to a saline treatment. (A) Protocol. All the plants were hydroponically grown for 5 weeks before being harvested. The nutrient solution was the standard one during the whole 5-week period (control plants), or was supplemented with 200 mM

NaCl either 48 h or 168 h (7 days) before the harvest. (B) *HmHKT2;1* transcript accumulation. Transcript accumulation (expressed per ng of RNA) was determined by qRT-PCR. Means \pm SE (three biological repetitions; for each biological repetition: three technical repetitions). Asterisks indicate significant differences (Student's *t*-test, $P \leq 0.05$) between Soliman and Kalbia plants.

Fig. 8. Potassium and sodium accumulation in plants grown in standard conditions or submitted to a saline treatment. All the plants were 5-week-old when harvested. The nutrient solution was the standard one (control plants) for the whole growth period, or was supplemented with 200 mM NaCl either 48 h or 168 h before plant sampling (protocol: see Fig. 7A). (A) K^+ accumulation ($\mu\text{mol}\cdot\text{plant}^{-1}$). (B) Na^+ accumulation ($\mu\text{mol}\cdot\text{plant}^{-1}$). Means \pm SE ($n = 4$). Asterisk: significant difference (Student's *t*-test, $P \leq 0.05$) between Soliman and Kalbia plants.

Fig. 9. Comparison of *Hordeum maritimum* Kalbia and Soliman plant biomass production in standard or saline conditions. All the plants were 5-week-old when harvested. The nutrient solution was the standard one (control plants) for the whole growth period, or was supplemented with 200 mM NaCl either 48 h or 168 h before plant sampling (protocol: see Fig. 7A). Means \pm SE ($n = 4$). Asterisk: significant difference (Student's *t*-test, $P \leq 0.05$) between *Hordeum maritimum* Soliman and Kalbia plants. Visual phenotype of the plant shoots: see Supplementary Fig. S8.

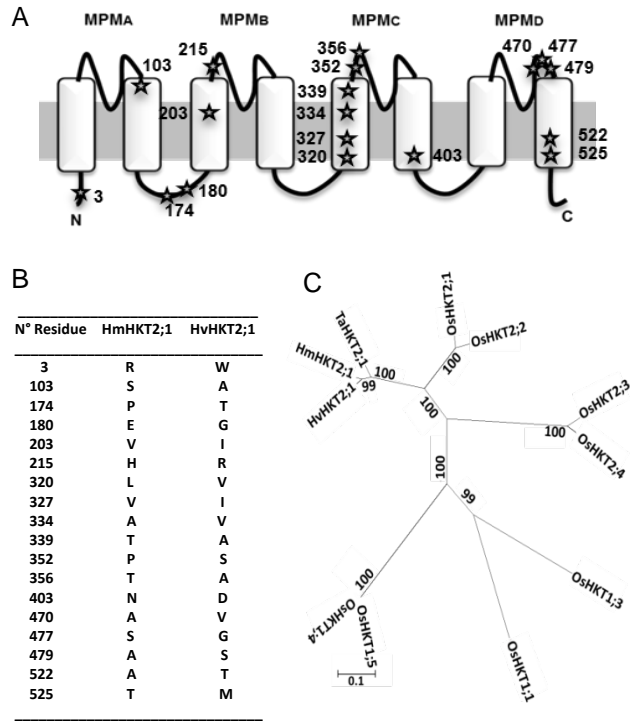


Fig. 1.

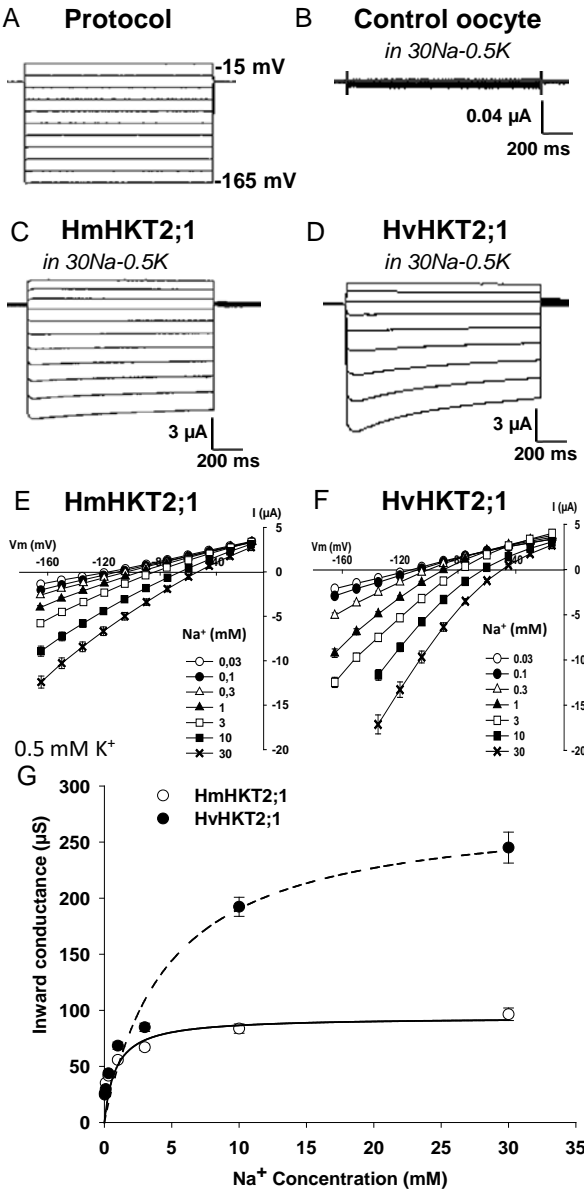


Fig. 2

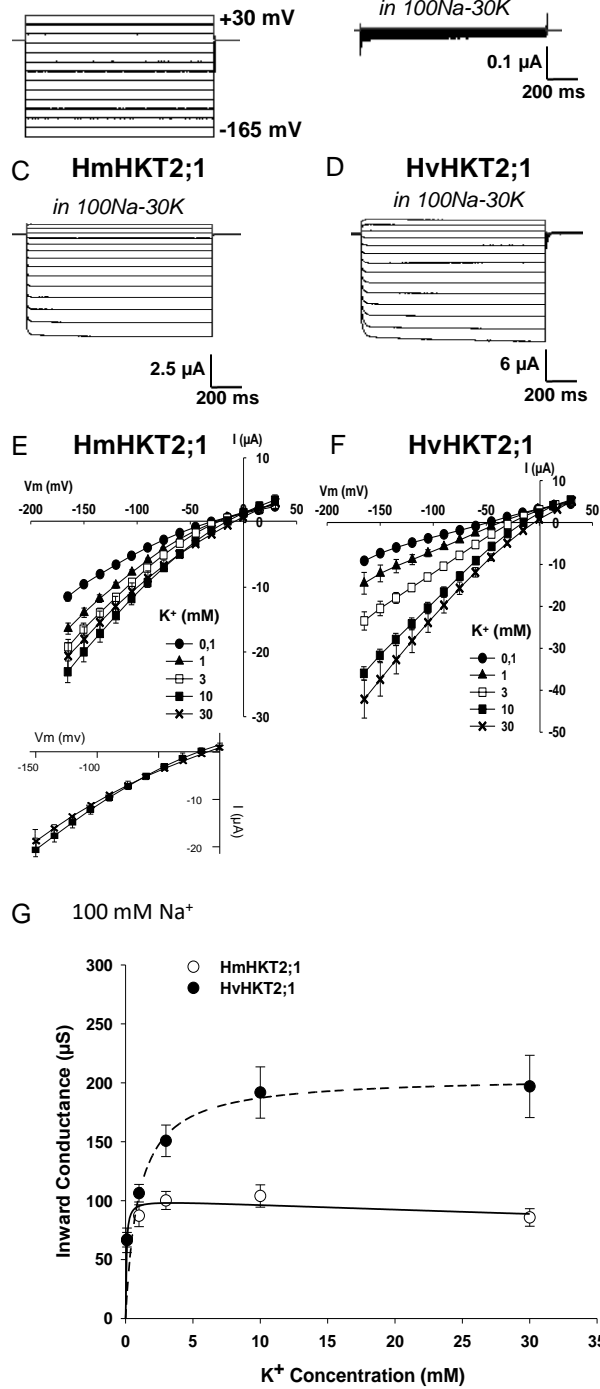
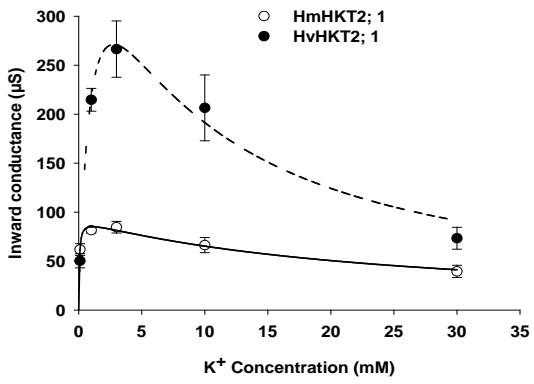


Fig. 3.

A 30 mM external Na⁺



B 0.5 mM external Na⁺

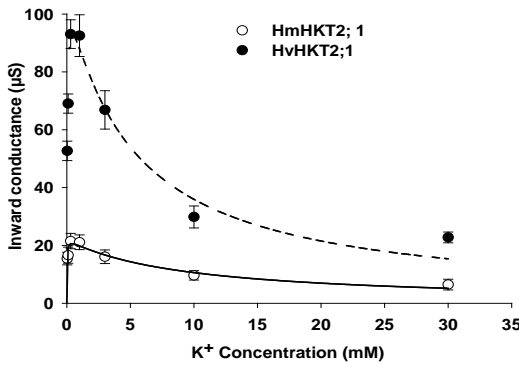


Fig. 4.

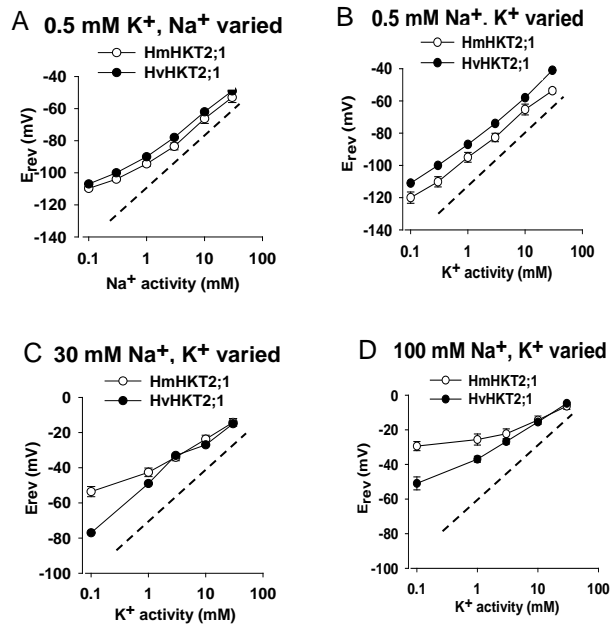


Fig. 5.

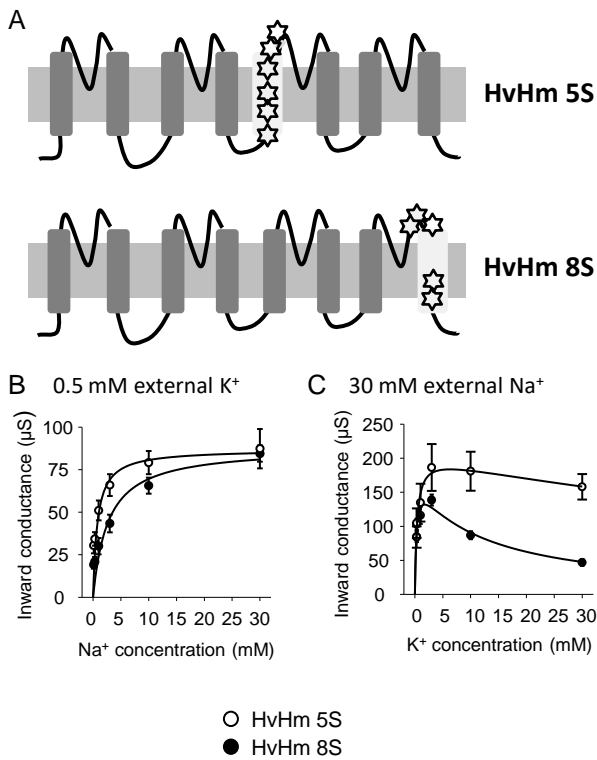


Fig. 6.

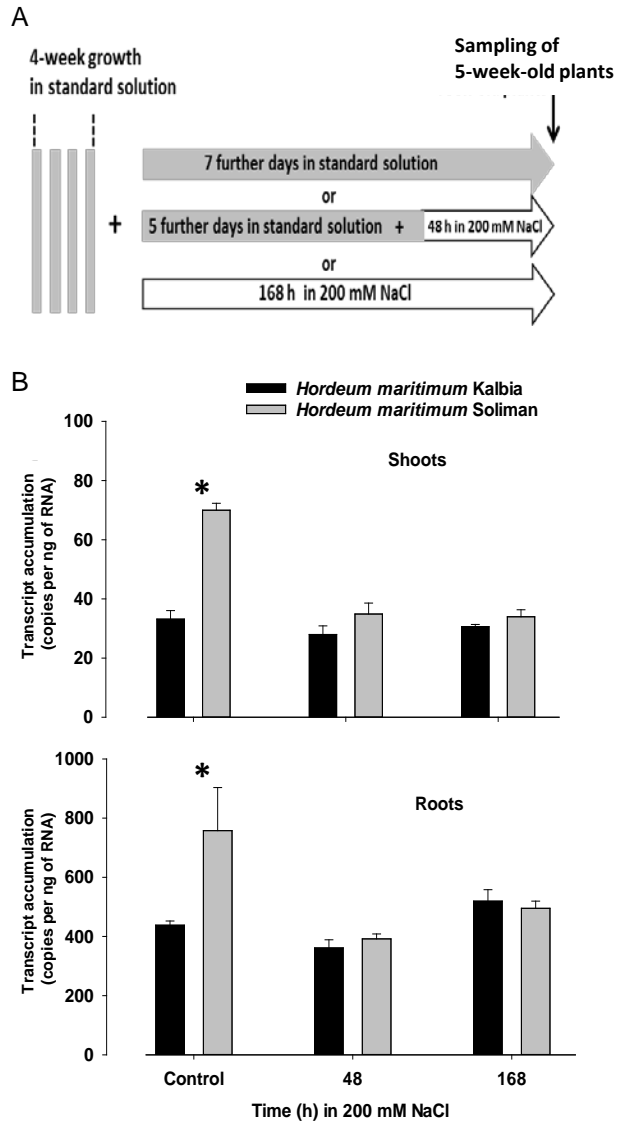


Fig. 7.

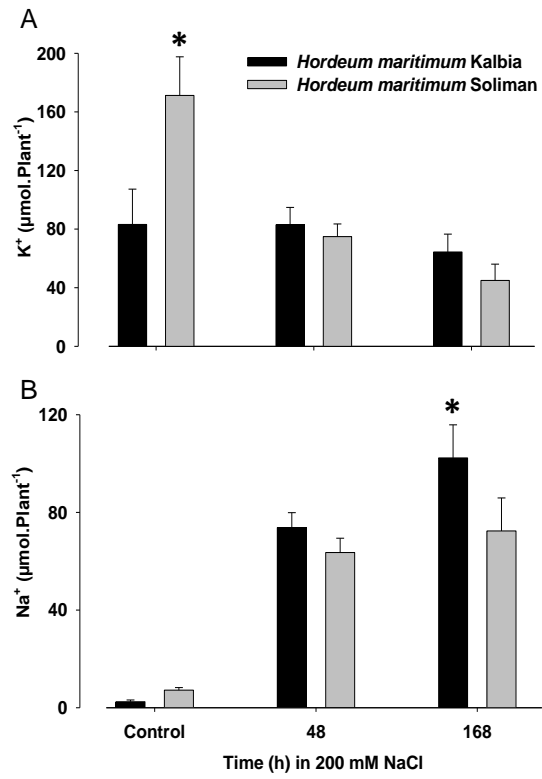


Fig. 8.

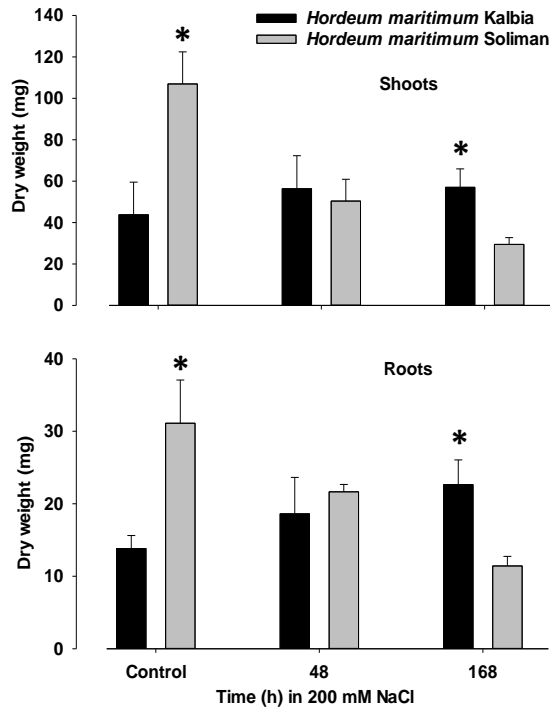


Fig. 9.